



AIAA 2002-5855

**Using Response Surface Metamodels to
Optimize the Aerodynamic Performance of
a High Speed Standoff Missile within a
Multi-Disciplinary Environment**

**Henry Won, Simon Levine, Holger Pfaender, and
Dr. Dimitri N. Mavris**

**Aerospace Systems Design Laboratory
School of Aerospace Engineering
Georgia Institute of Technology
Atlanta, GA**

**Aircraft Technology, Integration, and Operations (ATIO)
2002 Technical Forum**

**1-3 October 2002
Los Angeles, California**

Using Response Surface Metamodels to Optimize the Aerodynamic Performance of a High Speed Standoff Missile within a Multi-Disciplinary Environment

Henry Won,* Simon Levine,* Holger Pfaender,* and Dr. Dimitri N. Mavris†

Aerospace Systems Design Laboratory
School of Aerospace Engineering
Georgia Institute of Technology

Abstract

This report summarizes the feasibility of implementing a metamodel, consisting of Response Surface Equations (RSE), in a High Speed Standoff Missile (HSSM) multi-disciplinary mission analysis. The metamodel, which is a representation of a physics based engineering tool, is used to optimize the missile aerodynamic performance for any given mission. Each mission is defined as a function of the mission parameters. The optimization schemes use flight condition information and missile requirements from the upstream mission analysis, and find the optimum missile geometry parameters for that mission. The geometry parameters are then returned to the system analysis to complete the mission evaluation under optimal aerodynamic performance. The optimization scheme allows the variation of the missile geometry without increasing the number of runs in a parametric design study, such as a Design of Experiments (DOE).

Results are achieved for two modules, namely the fuselage aerodynamics and the tail fin aerodynamics. Metamodel optimization schemes were created and implemented into the modules. The transformed modules were tested to observe the behavior and accuracy of the schemes. Comparison is made between the optimal geometries found with and without the use of the metamodel. The comparison shows that the metamodel optimization returns similar results, and does so in a significantly shorter amount of time. In addition, the aerodynamic design spaces are analyzed in conjunction with the optimization behavior to predict possible problems in the optimization process. The use of the metamodel is shown to alleviate optimization problems such as multi-modal design spaces. The results indicate the usefulness and promise for the proposed metamodel optimization scheme for use in a large scale preliminary design analysis.

Copyright © 2002 by Henry Won, Simon Levine, Holger Pfaender, and Dimitri N. Mavris. Published by the American Institute of Aeronautics and Astronautics, Inc., with permission.
* Graduate Research Assistant, AIAA Student Member
† Boeing Professor for Advanced Design, School of Aerospace Engineering, Director, ASDL, Associate Fellow, AIAA.

Nomenclature

Λ_0	Fin leading edge sweep [deg]
c_r	Fin root chord [ft]
c_t	Fin tip chord [ft]
λ	Fin taper ratio (c_t/c_r)
b	Fin span [ft]
t/c	Fin thickness to chord ratio
c_{LE}	Fin leading edge kink location [%c]
c_{TE}	Fin trailing edge kink location [%c]
S	Fin planform area [sq ft]
M	Freestream Mach number
α	Angle of attack [deg]
Alt	Altitude [ft]
$\partial C_N / \partial \alpha$	Normal force coefficient curve slope
C_D	Drag coefficient

Background

Modern military aerospace design trends are requiring a more thought out preliminary design (PD) phase. The PD phase evaluates on a system level the performance of a concept, whether it be a component level modification or a completely new vehicle. Traditionally, the PD stage was passed quickly because our enemy was a well defined monolithic adversary¹, and designers had a "design for performance" attitude. This provided for well defined mission parameters and performance goals. Today, the enemy has changed to smaller rogue states, and designers have a "design for affordability" attitude.² The effect on the PD phase is that the mission requirements become less defined, and that the analysis must provide enough information to accommodate a more robust solution rather than a point performance design.

To accommodate the two aforementioned modifications on the PD phase, the PD engineer can no longer seek a single optimum solution. Instead, the necessity is to create a dependable analysis environment that will, in a sufficiently timely manner, address all the possibilities of changing mission parameters and design uncertainties on a module or component level. The viable solution is to perform a parametric study on the mission analysis through variation of

the mission requirements and design uncertainties. The effects should be apparent on the mission figures of merit with parametric variation on the vehicle component or module level. This requires the setup of a physics based, multi-disciplinary analysis. Figure 1 conceptually depicts such an analysis.

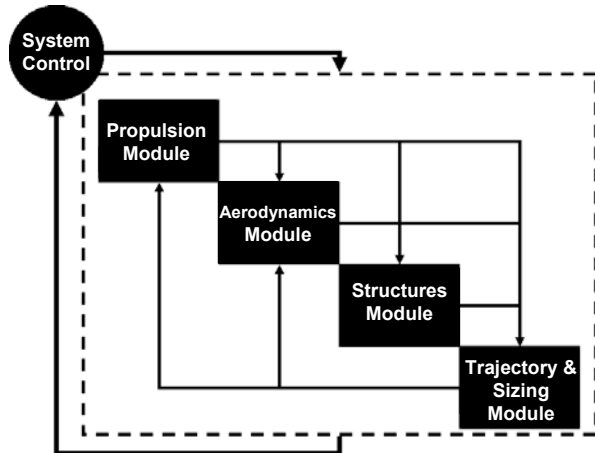


Figure 1 A generic multi-disciplinary design structure.

The system analysis is what is enclosed within the dashed line. Each of the boxes within the dashed line is a module of the system analysis. These modules perform the analyses of their specialty using physics based computations. Physics based computations, as opposed to regressions of historical trends, allow more “outside of the box” design analysis, where there is little or no historical data to rely on. The modules perform in the respective manner and pass the design and intermediate variables to the other modules. The arrows indicate the direction of data flow. Notice that the arrows below the boxes indicate back flow. These are points that may require iteration and convergence between modules. Setting up such an analysis is in itself its own discipline known as multi-disciplinary design analysis and optimization. It involves a mix of gaining expert knowledge in each discipline, finding a set of analysis tools that balances result accuracy or fidelity and run time, and setting up the modules in the optimum manner.

The circle in the diagram indicates the system control. The system control knows what is inside the dashed line simply as a “black box”. The system control acts as an operator and passes the “black box” a set of input variables, indicated by the thick arrow leading into the dashed box, and receives a set of mission figures of merit as an output of the mission analysis, indicated by the

arrow leading out of the dashed box. As a clarification, reference to the “system level” or “mission analysis” indicates that which is seen by the “system control”. “Module level” indicates that which is seen by any one of the individual analysis blocks within the dashed line.

To satisfy the need to examine a broad range of mission requirements, and to find a robust design, the system control needs to examine the mission analysis over a large design space. The design space dimensions are defined as the input design parameters, and the boundaries are defined by the ranges of those parameters that wish to be observed. These parameters include mission parameters, which typically map to the mission requirements, and also module level design variables. The final dimensions are the outputs of the analysis. Tools which are used to examine and visualize a vehicle design space include design space prediction profiles, contour plots, Monte Carlo simulations, and uncertainty analyses. These tools require a number of runs that easily reach into the 1000’s, hence the need for a timely system level analysis is eminent.

HSSM System Level Analysis

The authors completed a preliminary design system level analysis of a hypersonic High Speed Standoff Missile (HSSM), which specifically motivated the need to create more timely module level analysis methods. These module level methods would allow a more complete set of variables in the system level parametric analysis.

Joint efforts between several potential customers resulted in a RFP for a HSSM. The HSSM is a proposal to fulfill the need to strike time critical targets, such as mobile theatre ballistic missiles, with dwell times typically around 10 minutes. Deterministically, the RFP required a ship launched missile, deployable from a Vertical Launch System (20”x20”x256” with max launch capacity 3400 lbs), with no ejectables beyond 50 km radius of the ship. Outside of these determined requirements, the ranges of mission figures of merit are given in Table 1.

	Threshold	Standard	Goal
Cruise Mach	4	5	6
Time to Target	15 mins	10 mins	5 mins
Range	500 km	1000 km	1500km
Impact Speed	2000 ft/s	3000 ft/s	4000 ft/s

Table 1: HSSM mission requirements regime

The possible conceptual configurations were open ended, including the choice of four air breathing

engines. By initial analysis and evaluation of the tools at hand, the missile configuration chosen to parametrically model was a 2-D mixed compression inlet, liquid fuel ramjet, with cylindrical body, four axisymmetric rear tail fins, and a separate booster. The configuration is shown in Figure 2.



Figure 2: The HSSM Configuration

A computer integrated, physics based multi-disciplinary design analysis system was created to evaluate this missile configuration³. The analysis modules comprising the system level analysis were the inlet ramp, ramjet cycle, missile body aerodynamics, structural, stability, booster sizing, and cruise sizing. The run time of a single mission analysis averaged 8 minutes.

The system level DOE included four mission parameters that were mapped from the above four mission requirements. These four parameters were cruise range, cruise Mach number, ramjet takeover altitude, and ramjet takeover Mach number. The number of DOE variables was held at such a minimum because of the long run time of the system level analysis. Other design parameters, including the missile geometry were held constant at values decided by engineering judgment. The authors' desire to include the variation of more variables, specifically the missile geometry variables, in the preliminary design study lead to the idea of transforming the simple aerodynamic analyses into metamodel optimization schemes.

Aerodynamic Analysis Modules

Analysis Codes

Two aerodynamic analysis codes were used to determine the aerodynamic properties of the various missile body and tail configurations to be tested.

The first code used was the high speed aerodynamic analysis code S/HABP Mark V (Supersonic/Hypersonic Arbitrary Body Program).^{4,5} S/HABP is a standard hypersonic aerodynamic analysis code used in preliminary

design. It employs various hypersonic approximation methods to determine the aerodynamic metrics for the configuration to be studied. In this study, S/HABP was configured to use the Tangent Cone, Tangent Wedge, and Prandtl-Meyer Expansion high speed flow approximation methods. The Tangent Cone and Tangent Wedge methods were used for the windward side of the missile body and fins respectively. The Prandtl-Meyer Expansion method was used on the leeward side of both the missile body and fins.⁶ The model geometry is represented in S/HABP by a collection of rectangular panels. The pressure acting on each panel is calculated using the methods mentioned above, and forces are determined by multiplying this pressure by the panel area. S/HABP does not take into account interactions between the various panels of the model. However, this is correct in the limit of the hypersonic approximations employed by S/HABP. Consequently, each component (i.e. fin, fuselage) of the model can be analyzed separately.

In addition, the skin friction drag component of the collection of aerodynamic analysis codes known as BDAP (Boeing Design and Analysis Program) was used to supplement S/HABP by providing skin friction drag data. This program calculates skin friction drag using the turbulent flat plate theory method by near field drag calculation subroutine.⁷

The wireframe missile body and fin models used by these two codes were generated by using the airframe geometric modeling program RAM (Rapid Aircraft Modeler).⁸ The missile body and tail fins were modeled separately in order to perform the aerodynamic analyses of each of these two components independently.

All the codes used in the aerodynamic analysis were linked together using iSIGHT, a software package that automates manual design processes.⁹

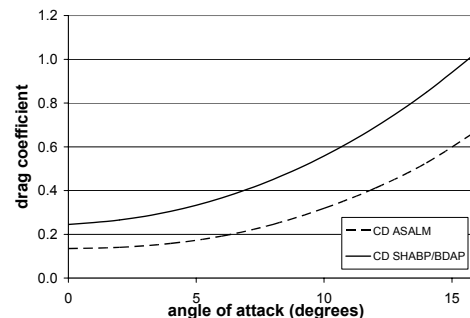


Figure 3: Actual and predicted values of the ASALM C_D at Mach 4

The two aerodynamic codes were preliminarily validated against data from the Advanced Strategic Air Launched Missile (ASALM), a 1970s Mach 4 ramjet missile. A simplified model of the ASALM was created in the Rapid Aircraft Modeler and tested against actual ASALM data¹⁰. The comparison is shown in Figure 3. This data, which is the drag coefficient at Mach 4, shows reasonable correlation to the ASALM data, and is not expected to be exact due to the simplicity of the created model.

Module Setup

Originally, the two separate aerodynamics modules, one for the missile body and the other for the tail fins, each used only the aerodynamic analysis setup shown in Figure 4. Each execution of the analysis requires a set of geometry and freestream condition inputs, and provides a set of desired aerodynamic metric outputs.

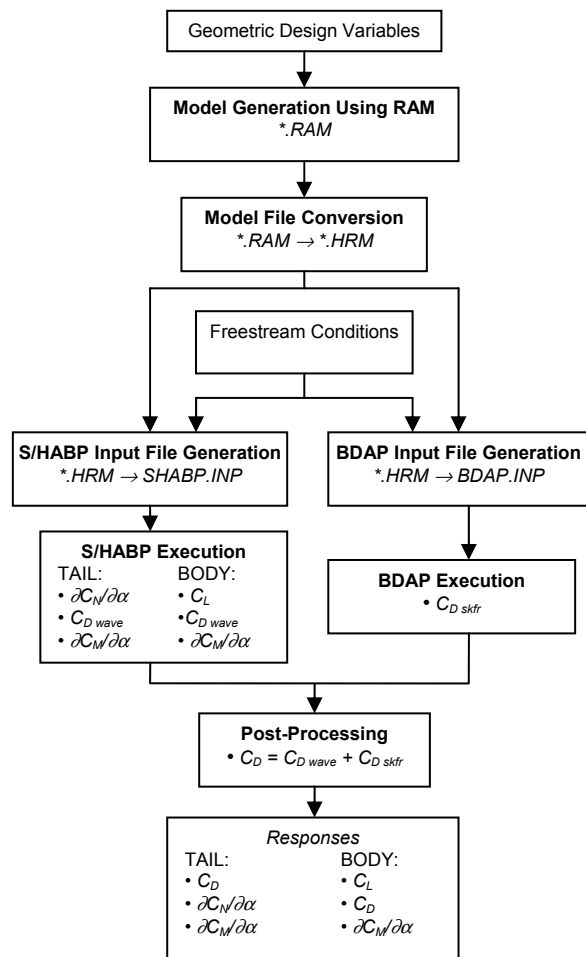


Figure 4: Aerodynamic Analysis Setup

Each aerodynamic analysis execution for the missile body returns lift and drag as a function of angle of attack, altitude, Mach number, and body geometry. For a given geometry, the missile body module utilized the analysis to create drag polars by repeating the analysis throughout the flight regime. The drag polars were later used in the trajectory module. In addition, the fuselage longitudinal stability derivatives were calculated at a single design point for later use in the tail sizing. The missile body module had a runtime of less than 30 seconds. This included a single execution of the RAM GUI, taking approximately 10 seconds, to save the missile geometry as a hermite file. Each aerodynamic analysis execution for a given tail fin geometry returns the tail fin longitudinal stability derivatives as well as the tail fin drag. This information was used to size the tail fins for longitudinal static stability. The tail fin module analysis had a runtime of approximately five seconds. Again, this included the single RAM GUI execution.

Aerodynamic Modules Transformations

Methodology

To reiterate, the focus of this paper is to describe and evaluate a method by which the authors, motivated to include variation of the HSSM geometry parameters in the parametric preliminary design study, transformed the deterministic aerodynamic modules into metamodel optimization schemes. This transformation has two distinct parts: 1) transforming the modules into ones that determine the optimal geometry variables, and 2) creation of response surface equations (RSE) to form the metamodel and replace the exact analysis of Figure 4 in the aerodynamics modules. Figure 5 conceptually depicts part one of the transformation.

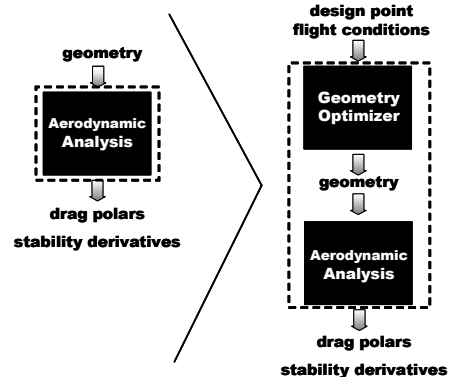


Figure 5: Conceptual Depiction of Missile Body Aerodynamic Module Transformation

The left side of the diagram shows the original missile body aerodynamics module (within the dashed lines), and the right side shows the modified aerodynamics module. The significance of this to the system level analysis is that the missile geometry is varied, but does not need to be included in system level parametric studies. The geometry can be optimized for aerodynamic performance within the given constraints (e.g. VLS constraints). Therefore, each mission can be analyzed with the optimal missile body geometry. In the original system level PD study, the geometry variables were held constant for all missions, so that while one mission may have benefited slightly due to the given geometry, another mission was degraded due to the given geometry. Analogously, the transformation described above can also be applied to the tail fin aerodynamic module.

To complete part 1 of the transformation, optimization schemes were created for the aerodynamic modules. These optimizations are of the generic form:

Given: c_i
 Vary: x_i
 Such that: $f(x_i)$ is optimal
 While: $g_j(x_i, c_i) \geq 0$
 $h_j(x_i, c_i) = 0$

where c_i are input conditions, x_i are missile geometry variables, $f(x_i)$ is an aerodynamic function of the geometry (e.g. drag), $g_j(x_i)$ are inequality constraints, and $h_j(x_i)$ are equality constraints.

Part 2 of the transformation is the creation of the aerodynamic analysis metamodel. This involves modeling the outputs of an exact analysis by a number of quadratic equations. These equations are known as response surface equations (RSE). Each RSE represents a particular aerodynamic metric of interest, and is a function of the same variable inputs as the exact analysis. The combination of RSEs that are created compose the metamodel. Each RSE is created through an n-dimensional quadratic statistical regression of data from the exact analysis within the design space. The data used in the regression is generated from a design of experiments (DOE). A DOE is a number of sets of predetermined input variables (experiments) which should capture the independent effects of the input variables and their interactions on the responses¹¹. The RSEs that result from the regression together replace the exact analysis. The benefits of using a metamodel in place of the exact analysis are

many: instantaneous runtime, ease of calculation, and predictable behavior. These benefits come at the expense of introducing regression error. The amount of regression error is based on the dissimilarity of the true output behavior to the quadratic equation.

Using the methodology described above, the transformation of an aerodynamic module into a metamodel optimization scheme was applied to the missile body and tail fin aerodynamic modules from the HSSM system analysis.

Missile Body Aerodynamics

The missile body aerodynamics module was transformed into the following optimization scheme:

Given: Mach number, altitude, inlet ramp geometry, missile weight, required volume
 Vary: fuselage height, fuselage width, fuselage length, curvature strength, angle of attack
 Such that: C_D is minimized
 While: lift – weight ≥ 0
 volume – volume required ≥ 0

This scheme optimizes the geometry, as will be defined in the following paragraphs, to reduce the drag at the conditions at the midpoint of the cruise section. The conditions at the midpoint are indicated by the given cruise Mach number, cruise altitude, and missile weight. The chosen scheme was determined to be the most compatible with the mission analysis. The volume requirement ensures that the missile can accommodate the volume of the fuel and the missile components. This alleviates the need to put minimum boundaries on any of the fuselage dimensions. The volume required is that at time of launch. The lift constraint ensures that the missile will produce enough lift to support the missile weight at the midpoint of the cruise section. The trajectory module downstream in the mission analysis flies at the α of the missile at given mission cruise altitude and Mach number such that the lift is equal to the weight. The desire is to minimize the drag where this equality occurs. Hence lift is calculated as opposed to C_L or L/D, because it gives a dimensional value. Using the lift necessitated including angle of attack in the list of optimizer parameters. As such, a given configuration was allowed to fly at any α that optimized its performance. This neglects the effects of angle of attack on the ramjet intake. Theoretically, the α chosen in the optimization will also be chosen in

the trajectory module, as that is where lift is equal to drag.

A metamodel was created to be used in the optimization process. The metamodel consists of RSEs of the missile lift, drag, and internal volume as a function of ten variables as listed in Table 2.

Parametric Variable	Range
<i>fuselage length</i>	12-14 ft
<i>fuselage height</i>	1.25-1.67 ft
<i>fuselage width</i>	1.25-1.67 ft
<i>bottom curvature strength</i>	0.83-1.71
<i>angle of attack</i>	0-9 degrees
<i>altitude</i>	80k-95k ft
<i>Mach number</i>	Mach 4-6
<i>inlet ramp length 1</i>	2.5-3.25 ft
<i>inlet ramp length 2</i>	1.1-1.3 ft
<i>inlet ramp angle 1</i>	12-12.5 degrees

Table 2: Missile Body Design Variables and Ranges

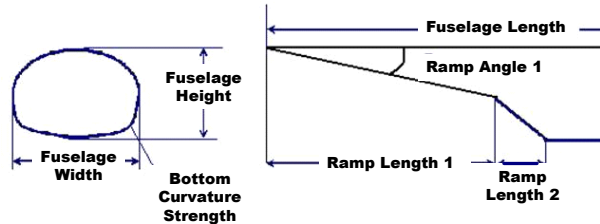


Figure 6: Missile body geometry defined.

The first five variables in Table 2 are varied by the optimization scheme, while the other five are input conditions and parameters. The input cruise Mach ranges are dictated by the mission requirements of Table 1. The altitude is dictated by the range of cruise altitudes chosen for the system level DOE. The inlet ramp angles include the ranges of values valid for these Mach numbers, as calculated by the inlet ramp module. The other five variables, with the exception of angle of attack, are missile body geometry variables and are depicted in Figure 6.

On the left is the body cross-section view of the missile and on the right is the nose side view. The curvature strength only affects the bottom half of the missile, and values are set such that when equal to 0.83, the cross-sectional shape is purely elliptical, and square on the bottom when set to 1.71.

To accommodate the ten variables, a 129 run Central Composite Response Surface Design (CCD) Design of Experiments was implemented

using the above variable ranges as high and low values. Figure 8 shows a sample from the 129 runs of the different sets of missile geometries included in the DOE. These experiments were run through the BDAP and S/HABP exact analysis setup of Figure 4. The resulting data was compiled in the JMP 5.0 statistical software package in order to complete the regression analysis.¹²



Figure 8: Side-view samples of geometries included in the 129 variable DOE.

RSEs were generated for the responses important to the optimization scheme, namely drag coefficient, lift, and internal volume. The three fits had small regression error, with the lift RSE having the most noticeable regression error. Figure 7 shows the prediction profiles of each response (rows) with respect to the five optimizable variables (columns). Mach number, altitude, ramp lengths, and ramp angle are all held constant at

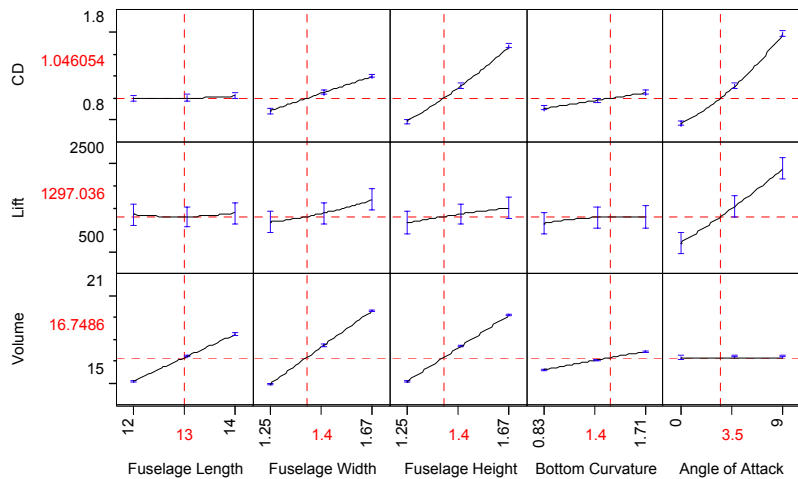


Figure 7: Fuselage Aerodynamic Prediction Profile

Mach 4, 80,000 ft, 2.9 ft, 1.2 ft, and 12.3 degrees respectively.

The prediction profile shows the expected value and gradient of the outputs at the chosen variable values. The chosen values are indicated by the vertical, dashed crosshairs. From this, an idea of how the optimizer will behave is apparent. For example, to minimize C_D the optimizer will move in the downhill direction of the C_D profiles. But, if the volume constraint is critical, the optimizer would first decrease the fuselage length, because it gives more volume with the least increase in C_D as indicated by the slope.

To test how well the metamodel optimization would perform, two setups were compared. The first setup was the metamodel optimization. The second setup used only part 1 of the transformation. Hence, both setups performed the same optimization. However, the first setup, the metamodel optimization, used the RSEs to calculate lift, C_D , and volume, while the second setup, the exact optimization, used the exact analysis to calculate these quantities.

The metamodel optimization scheme was implemented in MATLAB using the *fmincon* function, which is a sequential quadratic programming (SQP) technique. The stopping accuracy was set to $1E-10$. The exact analysis optimization scheme was a modified version of the original integrated iSIGHT setup of BDAP and S/HABP. iSIGHT was programmed to perform an SQP optimization of the aerodynamic analysis codes. The stopping accuracy was set to $1E-3$.

Results were compared between the exact optimization and metamodel optimization among a design space of flight conditions and missile requirements as listed in Table 3.

<i>Altitude</i>	<i>80k-95k ft</i>
<i>Mach</i>	<i>Mach 4-6</i>
<i>Weight</i>	<i>1000-1600 lbs</i>
<i>Required Volume</i>	<i>16 - 20 cubic ft</i>

Table 3: Range of conditions under which optimal geometry was calculated

Each of the ranges was split into four sections such that 256 points were run, all simulating possible runs of the system level DOE. Each of the 256 input conditions were run through the optimization scheme both with and without the metamodel implemented. The resulting data was 256 aerodynamically optimized configurations at the altitude and mach specified, and satisfying the given weight and volume requirements. Figure 9

shows the resulting data in a comparison of the optimum drag coefficient found using the exact analysis against that found using the metamodel.

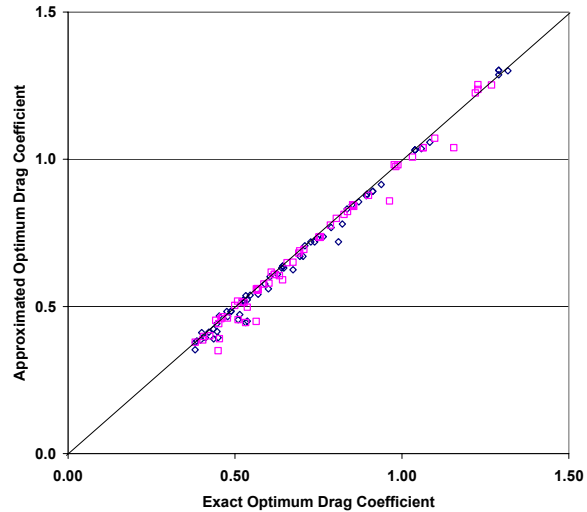


Figure 9: Exact vs. approximated optimum drag coefficient

The value of C_D shown for the metamodel optimization is the exact analysis calculation of C_D using the optimal geometry found in the metamodel optimization. Both methods found very similar optima for each of the 256 conditions.

Note that often the metamodel optimum gave a better C_D value than the exact optimum. There are two possibilities to consider: 1) the exact analysis solution is not the true optimum 2) the metamodel constraint values, although satisfied in the metamodel, were violating the exact values at the chosen geometry. The first possibility is addressed due to restrictions caused by the run time of the exact analysis. Because the exact analysis involved a GUI interface, RAM, the runtime was much longer. The average optimization required 50 runs through the aerodynamic analysis at 20 seconds per run. Hence, the stopping accuracy could not be further decreased (from $1E-3$), and the number of starting points was limited to one. A tradeoff between feasible run time and accuracy had to be made, giving an average optimization time of the exact analysis at 20 minutes. On the other hand, the metamodel optimization, which is optimizing a function that has a guaranteed and well defined global optimum (as do all constrained quadratic equations), could be run to very high accuracy ($1E-10$) in a very short time (less than 1 second). Hence, any optimum could be found to very high accuracy, and the space could be probed, via multiple starting points, to ensure the global optimum was found.

The second possibility to address is that, although the metamodel optimization found a more optimum C_D value, some constraints were violated due to the regression error in the metamodel. For example, an optimum configuration may have had just enough lift as required, but that lift would be the value as calculated by the RSE. If the metamodel optimum geometry configuration is rerun through the exact analysis, the lift may be calculated at a slightly different value. If the difference is negative, the metamodel optimum configuration would actually be violating the lift constraint (i.e. lift – weight < 0). If this is the case, it is important to quantify by how much the constraint is violated, and if that violation is of an acceptable level. To study this possibility, the values of lift and volume at the optimum drag geometry and flight conditions were recalculated using the exact analysis and the constraints were examined. Figure 10 shows the lift constraint against the corresponding difference in C_D values found by the metamodel and exact optimization schemes.

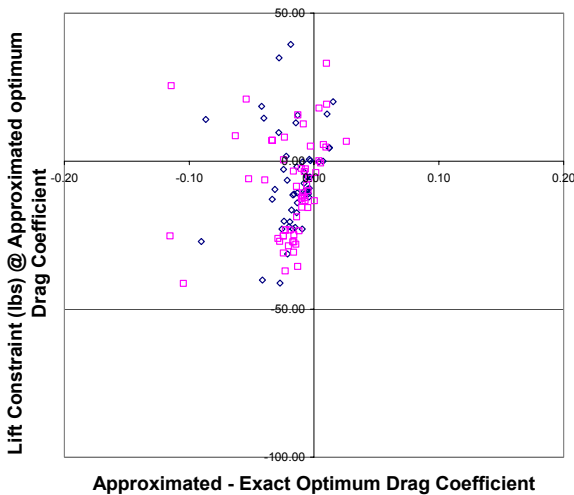


Figure 10: Examination of lift requirement violation

Note that a negative value on the y-axis is a constraint of the lift requirement and a negative value on the x-axis indicates that the metamodel found a more optimum C_D value. The graph indicates that the more optimum C_D values tend to violate the lift constraint, although by a relatively small amount (less than 50 lbs). Recall that the optimum configuration need not exactly satisfy the constraints, as downstream in the mission analysis, the trajectory module will still be able to fly the mission, and will only need a slightly higher α to create the extra 20 lbs or so amount of lift. The trajectory module will fly the mission in a near optimum manner, since a near optimum geometry

is found. Figure 11 shows a similar graph of the volume constraint violation using the metamodel.

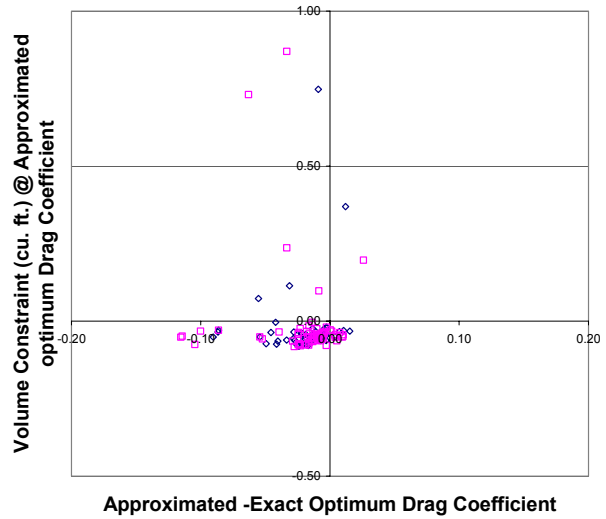


Figure 11: Examination of volume requirement violation

Again, there is a small amount of constraint violation (less than 0.1 cubic ft), but it is not as correlated to the more optimum metamodel C_D values as seen in the lift constraint violations. It seems that this is a small regression error in the metamodel fit and is small enough to be neglected.

In conclusion, the results shown here provide excellent support for the metamodel optimization methodology at hand. In most of the 256 optimization cases, the metamodel found as good or better optimal geometry, signified by the lesser C_D , with an acceptable level of constraint violation. The constraint violations were due to small regression error in the lift and volume RSEs. Otherwise, this bulk simulation of 256 missions showed the feasibility and benefits of implementing the metamodel optimization methodology. By determining the optimal missile body geometry, a given mission is flown under the best possible performance, thus creating a fair playing field when comparing a large number of missions, as such in a large scale PD analysis. As seen above, the metamodel optimization scheme will ensure this fair playing field.

Tail Fin Aerodynamics

In order to create the metamodel for the tail fins, it was first necessary to determine what independent design variables would define the fin configuration, and which responses were of interest. The independent design variables chosen consisted of the set of geometric variables

which together completely defined the geometry of the tail fins. A diagram of the fin defined by these variables is shown in Figure 12.

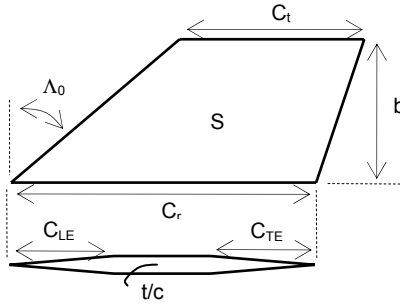


Figure 12: Definition of Tail Fin Geometry

As can be seen, the fin airfoil was defined as a truncated double wedge. The tip and root chords (C_t and C_r) were combined into one variable for taper ratio (λ). It was then possible to define the aerodynamic metrics of each tail fin as a function of six independent variables for given freestream conditions of Mach number, angle of attack, and altitude. For all tail fin configurations analyzed, the planform area, S , was held constant at 1 ft^2 , in order that this parameter did not dominate the fin aerodynamic metrics.

It was possible to select any aerodynamic property that was calculated by the aerodynamic codes as a response. However, for this study, the tail fin drag and the tail fin normal force curve slope ($\partial C_N / \partial \alpha$) were chosen as responses to be used in the optimization. The optimal tail fin was defined to be one with the maximum normal force curve slope and minimum drag. Maximizing $\partial C_N / \partial \alpha$ minimizes the required planform area for longitudinal static stability. Equations 1 and 2 below show the two RSEs defined for the tail fins.

$$C_D = f(\Lambda_0, \lambda, b, t/c, c_{LE}, c_{TE}) \quad (1)$$

$$\partial C_N / \partial \alpha = f(\Lambda_0, \lambda, b, t/c, c_{LE}, c_{TE}) \quad (2)$$

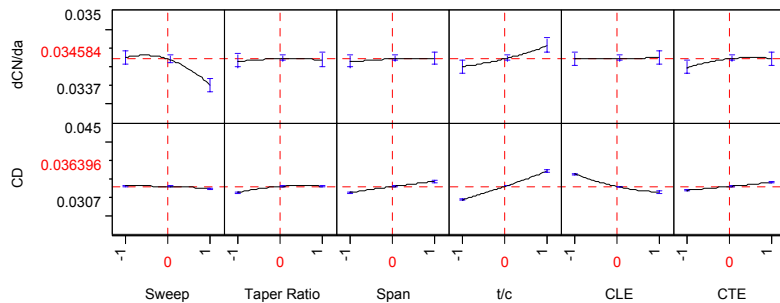


Figure 13: Fin Prediction Profiles

Creation of Response Surface Equations

A six variable Central Composite Response Surface Design (CCD) Design of Experiments was defined. This DOE consisted of 77 runs. The variable settings for each run were defined in non-dimensional form. That is, each variable had three possible settings: -1, 0, and 1. These non-dimensional values were converted to actual values using the design variable ranges shown in Table 4.

VARIABLE	LOWER	UPPER	
Λ_0	0	70	deg
λ	0	1	
b	0.75	1.25	ft
t/c	0.04	0.06	
C_{LE}	0.25	0.5	%c
C_{TE}	0.5	0.75	%c

Table 4: Design Variable Ranges

The analysis of Figure 4 was executed for each set of independent geometric design variables as defined by the DOE. From these analyses, the second-order Response Surface Equations were generated. Each box in Figure 13 represents partial derivatives of the responses (rows) with respect to one of the independent design variables (columns). That is, each box shows how a single variable influences a single response, while all other variables are held constant. The profiles are dependent on the settings of each of the variables. These prediction profiles are a very useful way to quickly visualize the effects of each variable on each response.

Optimization

In order to perform an optimization, it was first necessary to define an objective function to be minimized. The function chosen was the overall evaluation criterion equation of Equation 3.

$$OEC = \beta \times \frac{(\partial C_N / \partial \alpha)_{bl}}{(\partial C_N / \partial \alpha)} + \delta \times \frac{(C_D)}{(C_D)_{bl}} \quad (3)$$

The subscript "bl" denotes the baseline values of the responses. This equation is at its minimum when the normal force curve slope is at its maximum and the drag coefficient is at its minimum. The coefficients β and δ define the weighted importance of each metric to the overall evaluation criterion. These weights can be seen as being the subjective element to this analysis, since the relative importance of the two responses will impact the optimum

solution. The baseline fin was chosen to be one defined by the midpoint of all geometric variables. This fin is shown in Figure 14.



Figure 14: Baseline Fin

The Sequential Quadratic Programming method was used to optimize the OEC function. Since SQP is a path-based method, the optimizer will be able to converge on local minima only. Thus, if the design space is multimodal, the optimized design point found by SQP will be dependent on the initial starting point. Due to the shape of the design space, as can be seen visually in Figure 13 and Figure 15, the prediction profiles for sweep, taper ratio, and span can become convex at certain variable settings. Thus, when upper and lower bound constraints are introduced, the problem becomes multimodal since local minima are created at a number of locations along the constraints. Therefore, in order to use this type of optimization, one must begin the optimization at a number of different initial points, and then compare optima to see which is the true global optimum.

Alternatively, one could choose to use a stochastic method such as a Genetic Algorithm that is more suited to multimodal design spaces. Although this would be a more robust approach, it is also much more time intensive. However, the SQP path-based method was chosen for this analysis since it is relatively easy to implement, and is very efficient when used in conjunction with second-order polynomial RSEs. Since the run time of the SQP optimizations using RSEs is quite low, it was determined that using SQP with multiple starting points was an acceptable

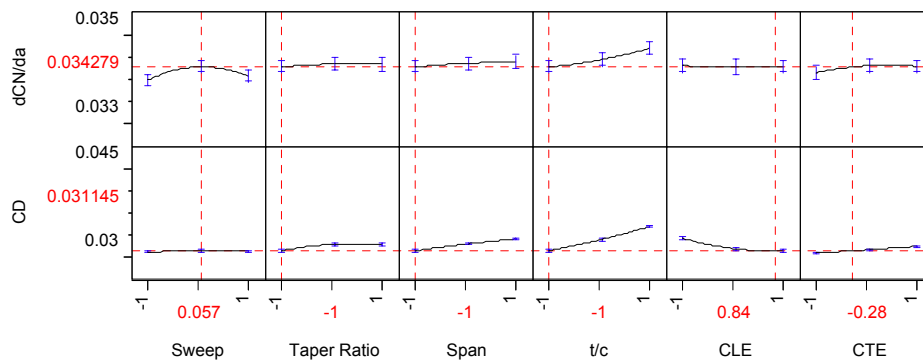


Figure 15: Prediction Profiles for Optimized Fin Configuration

solution.

The optimization was performed at Mach 5, an altitude of 100,000 ft, and an α of 5 deg. Note that the response values are for a pair of tail fins. Numerous starting points were used that spanned the entire design space. The global optimum found is detailed in Table 5. A diagram of this optimized fin is shown in Figure 16. For this analysis, the coefficients β and δ were set to 0.8 and 0.2 respectively. $\partial C_N/\partial \alpha$ was considered to be of more importance than C_D since the drag contribution of the tail fins to the overall missile was minimal compared to that of the missile body. The entire optimization process (65 individual optimizations) run time was approximately 3 min.

VARIABLE	OPTIMIZED VALUE	
Λ_0	37	deg
λ	0	
b	0.75	ft
t/c	0.04	
C_{LE}	0.48	%c
C_{TE}	0.59	%c
RESPONSE	OPTIMIZED VALUE	
$\partial C_N/\partial \alpha$	0.0343	(2 fins)
C_D	0.0311	(2 fins)

Table 5: Optimum Fin Configuration

This optimized design is at minimum taper ratio, minimum span, and minimum t/c. The leading edge sweep and kink locations were all a compromise between increasing the normal force curve slope and decreasing drag. The reasons for this design point being the optimum can clearly be seen in the prediction profiles in Figure 15. In these profiles, the variables are all set at their optimum values. For example, examining the prediction profile of $\partial C_N/\partial \alpha$ with respect to leading edge sweep, one can clearly see the maximum point on the profile is at 37 deg (0.57 normalized). One must keep in mind that this optimized

configuration is valid for the weights ($\beta=0.8$ and $\delta=0.2$) used in the objective function (OEC). For example, if more importance was given to the drag coefficient, and less to $\partial C_N/\partial \alpha$, the fin airfoil would tend to progress to a true wedge with maximum t/c at 50%.



Figure 16: Optimized Fin

For comparison purposes, a Genetic Algorithm optimization using the exact analysis (not the metamodel) was performed. The number of function calls was approximately equal to that of the SQP optimization. The GA optimization run time was 6 hours, 120 times as long as the metamodel optimization. The minimum objective function value obtained by the exact GA optimization was equal to that from the metamodel SQP optimization. The optimized values of the design variables obtained from each optimization were equal, except for leading edge sweep. In the GA optimization, the optimal Λ_0 was 13 deg. greater. This can be attributed to regression error in the metamodel.

Conclusion

In this study, optimization schemes were implemented for the two aerodynamic modules using exact analyses and metamodels based on the exact analyses. The metamodel optimization method results compared favorably to the exact analysis optimization results for both modules. The metamodel optimizations were significantly faster than the exact analysis optimizations, as much as 1000 times. Although some accuracy was lost in the use of the metamodels in place of the exact analyses, the benefits of relatively faster and simpler computations outweigh this loss of accuracy. This reduction in accuracy was considered to be acceptable in this preliminary design study.

Future work would include investigating methods to create metamodels with reduced regression error. Possibilities to reduce regression error include variable transformations, higher order models, and sectioned design spaces. Also, mixed model optimizations could be attempted. For example, starting the optimization with the metamodel and then switching to the exact analysis when the near optimum is obtained. Future work would also include analyzing the tail fin hinge moment, and including this in the fin optimization. As well, the implementation of these transformed aerodynamics modules containing metamodel optimization schemes into the overall

system level mission analysis would be the final determination of the methodology feasibility.

¹ Roth, B., Mavris, D., "Evaluation and Selection of Technology Concepts for a Hypersonic High Speed Standoff Missile." Presented at 2000 Missile Sciences Conference, Monterey, Ca, 2000.

2 Mavris, D.N., DeLaurentis, D.A., "Methodology for Examining the Simultaneous Impact of Requirements, Vehicle Characteristics, and Technologies on Military Aircraft Design," Presented at the 22nd Congress of the International Council on the Aeronautical Sciences (ICAS), Harrogate, England, August 27-31, 2000.

3 Ender, T., McClure, E., "Development of an Integrated Parametric Environment for Conceptual High Speed Missile Sizing ", AIAA-2002-5856.

4 Keith A. Burns et. al. Viscous Effects on Complex Configurations. Technical Report WL-TR-95-3060, McDonnell Douglas Aerospace, 1995.

5 A.E. Gentry et. al. The Mark IV Supersonic-Hypersonic Arbitrary Body Program. Technical Report AFFDL-TR-73-159, 1973. Volumes I, II, III.

6 M.Moore, J.Williams, Aerodynamic Prediction Rationale for Analyses of Hypersonic Configurations, 27th Aerospace Sciences Meeting, January 9-12, 1989/Reno, Nevada.

7 Middleton, W.D., Lundry, J.L.m Coleman, R.G., "A Computational System for Aerodynamic Design and Analysis of Supersonic Aircraft, Part 2: User's Manual," NASA, 1976.

8 J. R. Gloude mans and Paul Davis. Rapid Aircraft Modeler (RAM). Developed by Sterling Software for the NASA-Ames Systems Analysis Branch.

9 www.engineous.com

10 Fleeman, E. L. "Tactical Missile Design" American Institute of Aeronautics and Astronautics, Reston, VA 2001

11 Michael Montero, "Introduction to Design of Experiments", <http://kingkong.me.berkeley.edu/html/pres_asse ts/pdfs/fracfact2.pdf>, summer 2001.

12 www.jmp.com